Anisotropic transport properties of cerium Kondo compounds

S. M. M. Evans,* A. K. Bhattacharjee, and B. Coqblin
Laboratoire de Physique des Solides, Bâtiment 510, Université Paris–Sud, 91405 Orsay CEDEX, France
(Received 30 July 1991)

The anisotropy of transport properties, i.e., the electrical resistivity, the thermoelectric power, and the thermal conductivity, observed experimentally in single crystals of noncubic cerium Kondo compounds, is studied here theoretically in a model that takes into account both crystal-field and Kondo effects. At temperatures that are high compared with the Kondo temperature, we use perturbation theory on the Coqblin-Schrieffer Hamiltonian, and at low temperatures we use the slave-boson technique on the periodic Anderson Hamiltonian. We study also the effect of disorder and the resulting relation between the residual resistivity and the coefficient of the resistivity T^2 law. Detailed comparison with experiment is finally given and a reasonable agreement is obtained for cerium Kondo compounds, such as $CePt_2Si_2$, $CeCu_6$, or $CeAl_3$.

I. INTRODUCTION

Among rare-earth systems, cerium and ytterbium compounds are known to have an anomalous behavior. Cerium Kondo compounds have been extensively studied from both an experimental and theoretical point of view.[1] At sufficiently high temperatures, i.e., for temperatures larger than the Kondo temperature T_k and the overall crystal-field splitting, these compounds have a magnetic susceptibility which follows a Curie-Weiss law with a magnetic moment corresponding roughly to the Ce^{3+} trivalent ion or to the $4f^1$ configuration and show a decrease of the magnetic resistivity with increasing temperature, generally in $\log T$ in a given temperature range. At very low temperatures compared to T_k, cerium Kondo compounds are characterized by a heavy-fermion behavior giving rise to enormous values of the electronic specific-heat constant γ and the magnetic susceptibility χ. The strong competition between the Kondo effect itself and the Rudermann-Kittel interaction yields at low temperatures either a magnetic ordering in many compounds such as $CeAl_2$,[2] CeB_6,[3] $CeCu_2$,[4] or $CeInAg_2$,[5] which have a typical γ value of order 100 mJ/mole K^2, or a complex behavior, weakly or nonmagnetic with strong short-range magnetic correlations in compounds such as $CeAl_3$,[6] $CeRu_2Si_2$,[7] or $CeCu_6$,[8,9] which have a γ value of order 1000 mJ/mole K^2. On the other hand, the heavy-fermion compound $CeCu_2Si_2$ becomes superconducting below 0.6 K.[10]

The transport properties, namely the electrical resistivity,[11] the thermoelectric power,[12] and the thermal conductivity[13] of cerium Kondo alloys and compounds have been computed for the "high-temperature limit," i.e., for temperatures larger than the Kondo temperature T_k, within third-order perturbation theory on the so-called "Coqblin-Schrieffer Hamiltonian"[14] and a good agreement with experiments has been obtained. At low temperatures, the Fermi-liquid behavior $\rho = AT^2$ of the resistivity has been also derived by several theoretical approaches.[15–17]

Recently, the anisotropy of the transport properties in single crystals of cerium Kondo compounds has been studied both experimentally and theoretically.[18] Experimental evidence for anisotropy effects in single crystals has been found in the three transport properties of $CePt_2Si_2$,[18] in the resistivity of $CeAl_3$,[19] $CeCu_2Si_2$,[20] $CeCu_6$,[21,22] $CeRu_2Si_2$,[23] and $CeSi_x$,[24] and in the thermoelectric power of $CeCu_6$ (Ref. 22) and $CeRu_2Si_2$ (Ref. 23) single crystals. The resistivity of $CeCu_2Si_2$ and $CeAl_3$ is smaller along the c direction than perpendicular to it, in contrast to the case of $CePt_2Si_2$ while in the case of orthorhombic $CeCu_6$ both resistivity and thermopower curves are different along the three directions.[21,22] At very low temperatures, the resistivity of some heavy-fermion compounds behaves as T^2. However, there is not much available data on the anisotropic behavior of the resistivity in single crystals at very low temperatures. The resistivity of $CePt_2Si_2$ is anisotropic, but there is no evidence for a T^2 behavior.[24] In the case of a $CeAl_3$ single crystal, the resistivity behaves as $\rho = AT^2$ along the c axis and perpendicular to it and the ratio $A_\parallel / A_\perp$ of the T^2 coefficients is of order 0.4.[19] The low-temperature resistivity of $CeCu_6$ single crystals has been also measured by several authors;[21,22,25] a $\rho = AT^2$ law has been obtained along the three directions x,y,z, although the measured values for the A_i coefficients are slightly different according to the different measurements.[21,25] Finally, the residual resistivity ρ_0, measured at the lowest possible temperature, is generally very large and this large value is connected to the heavy-fermion character; moreover, the residual resistivity is also anisotropic in single crystals of cerium compounds such as $CeAl_3$, $CeRu_2Si_2$, or $CeSi_{1.86}$.

The purpose of the present paper is to present a theoretical model, based on the resonant scattering mechanism including crystal-field effects and taking into account the anisotropy of the conduction-electron relaxation rate, in order to explain the large anisotropy observed in the electrical resistivity, thermoelectric power, and thermal conductivity of noncubic cerium Kondo compounds. Thus, in Sec. II, we will first present very briefly the calculation of the anisotropic properties within

the third-order perturbation theory model, valid for temperatures larger than the Kondo temperature T_k and we will apply it to both cerium and ytterbium Kondo compounds. Then, in Sec. III, we will present in detail the calculation of the low-temperature transport properties performed within the slave-boson approach and we will discuss the effect of impurity scattering. In Sec. IV, we will study the anisotropy of the residual resistivity ρ_0 and its relation with the coefficient A of the T^2 term in the resistivity for an alloy or an imperfect lattice. Finally, in Sec. V, we will discuss the application of our model to cerium (or ytterbium) Kondo compounds. In the present paper, we limit ourselves to the study of transport properties and we do not present any calculation of the magnetic susceptibility[27] and NMR data[28] in cerium Kondo compounds, which are already published elsewhere.

II. THE PERTURBATION THEORY MODEL FOR THE ANISOTROPY OF TRANSPORT PROPERTIES

We present here the theoretical calculation of the anisotropic transport properties within the effective exchange Hamiltonian (the so-called "Coqblin-Schrieffer Hamiltonian"[14] in perturbation theory up to third-order in exchange integrals. We give here only the main assumptions and results, since some partial accounts[18,26] of this calculation have been already reported, and moreover we present also a simple extension to the case of ytterbium compounds. This calculation is valid for Kondo compounds and for temperatures larger than the Kondo temperature T_k.

The effective exchange Hamiltonian for the $4f^1$ configuration of cerium is written as[11,14]

$$H=-\sum_{\substack{k,k'\\M,M'}} J_{MM'}c^*_{k'M'}c_{kM}(c^*_M c_{M'}-\delta_{MM'}\langle n_M\rangle) + \sum_{\substack{k,k'\\M}} \mathcal{V}_{MM}c^*_{k'M}c_{kM} \tag{1}$$

in the usual notation: c^*_M is the creation operator for the eigenfunction of $l=3$, $s=\frac{1}{2}$, $j=\frac{5}{2}$ and of energy E_M relative to the Fermi level and c^*_{kM} is the corresponding creation operator for the conduction-electron partial wave function. The exchange integrals $J_{MM'}(<0)$ are given by

$$J_{MM'}=\frac{|V_{kf}|^2}{2}\left[\frac{1}{E_M}+\frac{1}{E_{M'}}\right]. \tag{2}$$

There are certainly several origins for the observed anisotropy, but we will show that the Hamiltonian (1) yields a large anisotropy in transport properties. Another calculation using the self-consistent ladder approximation has been also performed to compute the electrical resistivity[29] and the thermoelectric power.[30]

Our previous calculations[11–13] of the transport properties have been always performed for polycrystals and we have there approximated the relaxation time of a conduction electron by an isotropic average over the different $\mathbf{k}$ directions of the conduction electrons. In the case of a single crystal, we compute the transport properties along the principal axes i and we must calculate the relaxation time $\tau_{\mathbf{k}\sigma}$ for a conduction-electron plane wave of wave vector $\mathbf{k}$ and spin σ, which turns out to be highly anisotropic. The classical formulas for the electrical conductivity $\sigma=1/\rho$, thermal conductivity K, and thermoelectric power S can then be written, for each direction i, as

$$\sigma=1/\rho=e^2K_0\ , \tag{3}$$

$$K=\frac{1}{T}\left[K_2-\frac{(K_1)^2}{K_0}\right], \tag{4}$$

$$S=\frac{1}{eT}\frac{K_1}{K_0}\ , \tag{5}$$

where the integrals K_n (written in the following K^i_n for each direction i) are defined by

$$K^i_n=\frac{1}{8\pi^3}\int\left[\frac{\partial\varepsilon_{\mathbf{k}}}{\hbar\partial\mathbf{k}_i}\right]^2\left[-\frac{\partial f_{\mathbf{k}}}{\partial\varepsilon_{\mathbf{k}}}\right]\varepsilon^n_{\mathbf{k}}(\tau_{\mathbf{k}\uparrow}+\tau_{\mathbf{k}\downarrow})d\mathbf{k}\ . \tag{6}$$

$\varepsilon_{\mathbf{k}}$ is the conduction-electron energy and $f_{\mathbf{k}}$ the Fermi-Dirac distribution. The relaxation time $\tau_{\mathbf{k}\sigma}$ is given here by

$$\frac{1}{\tau_{\mathbf{k}\sigma}}=\sum_{\mu}|\langle\mathbf{k}\sigma|k\mu\rangle|^2\frac{1}{\tau_{k\mu}} \tag{7}$$

as a function of the partial relaxation times $\tau_{k\mu}$ where the partial wave $|k\mu\rangle$ corresponds to one of the eigenfunctions in presence of the crystalline-field effect.

Thus, according to Refs. 11 and 18, $\tau_{k\mu}$ is given by

$$\frac{1}{\tau_{k\mu}}=\frac{mkv_0c}{\pi\hbar^3}(R_{k\mu}+S_{k\mu})\ . \tag{8}$$

m, v_0, and c are, respectively, the mass of the conduction electrons, the considered volume and the cerium concentration. We have also[18]

$$R_{k\mu}=\mathcal{V}^2_{\mu\mu}-|J_{\mu\mu}|^2\langle n_\mu\rangle^2+\sum_{\mu'}\frac{|J_{\mu\mu'}|^2\langle n_{\mu'}\rangle}{1-f_k(1-e^{\beta(E_\mu-E_{\mu'})})}\ , \tag{9}$$

$$S_{k\mu}=2\sum_{\mu' m}J_{\mu\mu'}J_{m\mu}J_{m\mu'}\langle n_{\mu'}\rangle(1-\delta_{m\mu}\delta_{m\mu'}) \times\frac{g(\varepsilon_k+E_m-E_\mu)}{1-f_k(1-e^{\beta(E_\mu-E_{\mu'})})} -2|J_{\mu\mu}|^2(\mathcal{V}_{\mu\mu}+J_{\mu\mu}\langle n_\mu\rangle) \times\sum_m(\langle n_\mu\rangle-\langle n_m\rangle)g(\varepsilon_k+E_m-E_\mu)\ . \tag{10}$$

In general, the partial wave function $|k\mu\rangle$ (or the corresponding $4f$ eigenfunction $|\mu\rangle$ in the presence of crystal-field effects) is a linear combination

$$|k\mu\rangle=\sum_M a_{M\mu}|kM\rangle \tag{11}$$

of the elementary wave functions $|kM\rangle$ with $M=\pm\frac{1}{2}$,

$\pm\frac{3}{2}$, $\pm\frac{5}{2}$ in the case of cerium compounds and with $M=\pm\frac{1}{2}$, $\pm\frac{3}{2}$, $\pm\frac{5}{2}$, $\pm\frac{7}{2}$ in the case of ytterbium compounds. Then we insert (11) in expression (7) and the weight of the partial wave $|kM\rangle$ inside the plane wave $|\mathbf{k}\sigma\rangle$ is given by (with $\sigma=\pm\frac{1}{2}$)

$$|\langle \mathbf{k}\sigma|kM\rangle|^2=4\pi\left[\frac{7-4\sigma M}{14}\right]|Y_3^{M-\sigma}(\Omega_{\mathbf{k}})|^2 . \quad (12)$$

The anisotropy in the transport properties comes from the angular integration over $\Omega_{\mathbf{k}}$ in (6), which gives different results for the different directions. In order to perform the integration over $\Omega_{\mathbf{k}}$ we write k_x^2, k_y^2, and k_z^2 as functions of spherical harmonics, and after performing the integration of the products of spherical harmonics, we get different results for the three integrals K_n^x, K_n^y, and K_n^z. We then proceed, as usual, for the calculation of the transport properties and in order to invert the relaxation times, we use the third-order perturbation approximation, which yields values $R_\mu=R_{k\mu}$ and $R=\sum_\mu R_\mu$ independent of k.[11] Detailed calculations can be found elsewhere.[18,26]

Thus, the electrical resistivity ρ_i along the i direction is given by

$$\rho_i=\frac{3m_i^2\pi v_0 c}{2e^2\hbar^3k_F^2}\left[R+S^{(0)}-\sum_{\mu(>0)}(a_i\xi_\mu^{20}+b_i\xi_\mu^{2+})(R_\mu+\mathcal{S}_\mu^{(0)})\right] . \quad (13)$$

The thermoelectric power S_i along the i direction is given by

$$S_i=\frac{1}{eT}\frac{1}{R}\left[S^{(1)}-\sum_{\mu(>0)}(a_i\xi_\mu^{20}+b_i\xi_\mu^{2+})\mathcal{S}_\mu^{(1)}\right] . \quad (14)$$

The thermal conductivity K_i along the i direction is finally given by

$$K_i=\frac{2\pi k_F^2\hbar^3k_B^2}{9m_i^2v_0c}\frac{T}{R}\left[1-\frac{3S^{(2)}}{\pi^2R(k_BT)^2}-\sum_{\mu(>0)}(a_i\xi_\mu^{20}+b_i\xi_\mu^{2+})\frac{1}{R}\left[R_\mu+\frac{3\mathcal{S}_\mu^{(2)}}{\pi^2(k_BT)^2}\right]\right] , \quad (15)$$

where

$$S^{(n)}=\sum_\mu \mathcal{S}_\mu^{(n)} , \quad (16a)$$

$$\mathcal{S}_\mu^{(n)}=\int\left[-\frac{\partial f_{\mathbf{k}}}{\partial\varepsilon_{\mathbf{k}}}\right]\varepsilon_{\mathbf{k}}^n S_{k\mu}d\varepsilon_{\mathbf{k}} , \quad (16b)$$

and

$$a_x=a_y=\tfrac{2}{35} , \quad a_z=-\tfrac{4}{35} , \quad (17a)$$

$$b_x=\tfrac{1}{35} , \quad b_y=-\tfrac{1}{35} , \quad b_z=0 . \quad (17b)$$

The two coefficients ξ_μ^{20} and ξ_μ^{2+} are characteristic of the crystal-field effects and they are different in the two cases of cerium and ytterbium.

For cerium compounds, we have

$$\xi_\mu^{20}=\sum_M(M+\tfrac{7}{2})(M+\tfrac{5}{2})(\tfrac{3}{2}-M)(a_{M,\mu}^2+a_{-M,\mu}^2) , \quad (18a)$$

$$\xi_\mu^{2+}=9\sum_M[(M+\tfrac{7}{2})(M+\tfrac{9}{2})(M-\tfrac{3}{2})(M-\tfrac{5}{2})]^{1/2}\times(a_{M,\mu}a_{M+2,\mu}+a_{-M,\mu}a_{-(M+2),\mu}) \quad (18b)$$

and for ytterbium compounds,

$$\xi_\mu^{20}=\sum_M(\tfrac{7}{2}-M)(M+\tfrac{5}{2})(\tfrac{3}{2}-M)(a_{M,\mu}^2+a_{-M,\mu}^2) , \quad (19a)$$

$$\xi_\mu^{2+}=-5\sum_M[(M+\tfrac{11}{2})(M+\tfrac{9}{2})(M-\tfrac{5}{2})(M-\tfrac{7}{2})]^{1/2}\times(a_{M,\mu}a_{M+2,\mu}+a_{-M,\mu}a_{-(M+2),\mu}) . \quad (19b)$$

We see that the anisotropy disappears in cubic crystals and that the basal plane anisotropy disappears in hexagonal or tetragonal crystal structures. The present calculation has been successfully applied to the anisotropic transport properties of cerium Kondo compounds, in particular to the three transport properties of $CePt_2Si_2$,[18] and to the electrical resistivity and the thermoelectric power of $CeCu_6$;[26] thus, we will not discuss this point here. On the other hand, there are presently no available data on anisotropy effects in ytterbium Kondo compounds, but the present calculation could give an explanation of such possible effects in noncubic ytterbium based single crystals.

III. THE SLAVE-BOSON APPROACH FOR ANISOTROPIC TRANSPORT PROPERTIES AT LOW TEMPERATURES

A. The conduction electron self-energy

The anisotropy of the electrical resistivity has been also observed experimentally at low temperatures with respect to the Kondo temperature T_k and in a few cases, namely $CeAl_3$ and $CeCu_6$, a $\rho_i=A_iT^2$ law has been deduced with different coefficients A_i for the resistivity measured along the different principal axes i.

The previous perturbation theory treatment does not work at all below T_k and, in order to describe the anisotropy of the transport properties at low temperatures, we consider here the slave-boson approach to the periodic Anderson model including crystal-field effects in noncubic structures. To calculate the resistivity in the limit $T\rightarrow 0$, we relate the scattering rate $1/\tau$ to the conduction-electron self-energy, which we compute from the boson fluctuations around the mean-field solution.[16]

As in the high-temperature limit, in order to derive the anisotropy, it is important to include the correct $\mathbf{k}$ and spin dependence for the hybridization matrix element. We calculate here the anisotropic transport properties first for a pure lattice. However, the residual resistivity, ρ_0 is large in cerium Kondo compounds and we introduce the effect of disorder to account for it. In a first step, we introduce an isotropic and temperature-independent scattering rate resulting from disorder purely on the conduction-electron sites. These calculations will be presented in the present section. On the contrary the problem of the f-electron disorder leading to a relation between the anisotropy of ρ_0 and that of the coefficient of the T^2 law of the resistivity will be discussed in the next section.

Let us present now the calculation of the conduction-electron self-energy performed within the slave-boson approach. The periodic Anderson model including crystal-field effects in the limit $U\rightarrow\infty$ and for a large spin-orbit coupling, can be rewritten, using the slave-boson approach, in the usual form:[16,31–33]

$$H=\sum_{k,\sigma}\varepsilon_{\mathbf{k}}c^{*}_{\mathbf{k}\sigma}c_{\mathbf{k}\sigma}+\sum_{i,\mu}E_{\mu}f^{*}_{i\mu}f_{i\mu}+\sum_{k,i,\sigma,\mu}[V_{\mu\sigma}(\mathbf{k})e^{i\mathbf{k}\cdot\mathbf{R}_i}c^{*}_{\mathbf{k}\sigma}f_{i\mu}b^{*}_{i}+\text{H.c.}]+\sum_{i}i\lambda_i(n^{i}_{f}+n^{i}_{b}-1)\ . \tag{20}$$

The $4f$ electrons are taken to have a degeneracy $N=2j+1$, which is then split by the crystal field to give three doublets with energies E_0, $E_1=E_0+\Delta_1$, and $E_2=E_0+\Delta_2$ in noncubic cerium Kondo compounds. The μ values denote the eigenstates of the crystal field, and in general they are linear combinations of the M states, with $M=\pm\frac{1}{2},\pm\frac{3}{2},\pm\frac{5}{2}$ in the case of cerium, as explained in the preceding section. For the conduction band, we use the $|\mathbf{k}\sigma\rangle$ representation for plane waves of wave vector $\mathbf{k}$ and spin σ. Thus, the hybridization matrix element is of the form

$$V_{\mu\sigma}(\mathbf{k})=V\langle\mathbf{k}\sigma|k\mu\rangle\ . \tag{21}$$

$|k\mu\rangle$ is given by (11) as a function of $|kM\rangle$ and we can write

$$\langle\mathbf{k}\sigma|kM\rangle=\sqrt{2\pi(7-4\sigma M)/7}\,Y_3^{M-\sigma}(\hat{\mathbf{k}})\ , \tag{22}$$

where $Y_3^m(\hat{\mathbf{k}})$ is the spherical harmonic for $l=3$ and m values and the term in (22) before the spherical harmonic is the Clebsch-Gordan coefficient for spin-orbit coupled states with $j=\frac{5}{2}$ and $l=3$. The constraint $n^{i}_{f}+n^{i}_{b}=1$ is enforced on each site by the Lagrange multipliers $i\lambda_i$, where n^{i}_{f} is the total number of f electrons on site i and n^{i}_{b} the number of slave bosons on site i.

Following Rasul and Desgranges,[31] we can write the partition function in terms of functional integrals. Performing a local gauge transformation, $b_i=r_ie^{i\theta_i}$ and changing $f_{i\mu}$ to $f_{i\mu}e^{i\theta_i}$ have the effect of shifting λ_i to $\lambda_i+\theta_i$, thus promoting λ_i from the state of a Lagrange multiplier to that of a boson field. In the usual "mean-field" approximation, we replace r_i and λ_i by their average values and the properties calculated are equivalent to those found using an effective hybridization Hamiltonian in which both the hybridization and the f-level energy are renormalized:

$$H=\sum_{\mathbf{k},\sigma}\varepsilon_k c^{*}_{\mathbf{k}\sigma}c_{\mathbf{k}\sigma}+\sum_{i,\mu}\varepsilon_{f\mu}f^{*}_{i\mu}f_{i\mu}+\sum_{k,i,\sigma,\mu}[\tilde{V}_{\mu\sigma}(\mathbf{k})e^{i\mathbf{k}\cdot\mathbf{R}_i}c^{*}_{\mathbf{k}\sigma}f_{i\mu}+\text{H.c.}]+\sum_{i}i\lambda(r^2-1)\ , \tag{23}$$

where $\tilde{V}_{\mu\sigma}(k)$ is still given by (21) as a function of $\tilde{V}=rV$ and $\varepsilon_{f\mu}=E_\mu+i\lambda$. r and $i\lambda$ are the mean-field parameters, which are determined by minimizing the free-energy. This gives $r^2=1-n_f$, where n_f is the mean number of $4f$ electrons per site. The effective hybridization becomes small in the Kondo limit ($n_f\rightarrow 1$). There are three renormalized $4f$ energies ε_{f0}, ε_{f1}, and ε_{f2}; ε_{f0} is small in the Kondo limit and, for large crystal fields, gives the energy scale or "Kondo temperature" for the system.

It is convenient to define linear combinations of f_μ and $f_{\mu'}$ where μ and μ' form the doublet with energy ε_{fn}, which hybridize with conduction electrons of a given spin:

$$f_{n\sigma}=\frac{1}{(|V_{\mu\sigma}|^2+|V_{\mu'\sigma}|^2)^{1/2}}(V_{\mu\sigma}f_\mu+V_{\mu'\sigma}f_{\mu'})\ , \tag{24}$$

where $n=0,1,2$ runs over the three f electron doublets. We can now write the Hamiltonian (23) as

$$H=\sum_{\mathbf{k},\sigma}\varepsilon_{\mathbf{k}}c^{*}_{\mathbf{k}\sigma}c_{\mathbf{k}\sigma}+\sum_{i,n,\sigma}\varepsilon_{fn}f^{*}_{in\sigma}f_{in\sigma}+\sum_{\mathbf{k},i,\sigma,n}[\tilde{V}h_n(\mathbf{k})e^{i\mathbf{k}\cdot\mathbf{R}_i}c^{*}_{\mathbf{k}\sigma}f_{in\sigma}+\text{H.c.}]+i\sum_{i}\lambda(r^2-1)\ , \tag{25}$$

where

$$h_n(\mathbf{k})=(|V_{\mu\sigma}(\mathbf{k})|^2+|V_{\mu'\sigma}(\mathbf{k})|^2)^{1/2}/V\ .$$

To go beyond the mean-field limit, we need to include fluctuations in the boson field. Fluctuations in the amplitude δr_i couple to the hybridization and fluctuations in the phase velocity $\delta\lambda_i$ cause the f-level energy to fluctuate. We obtain an interaction term of the form

$$H_{\text{int}}=\sum_{i,k,n,\sigma}[\delta r_i(\tau)Vh_n(\mathbf{k})c^{*}_{\mathbf{k}\sigma}f_{in\sigma}e^{i\mathbf{k}\cdot\mathbf{R}_i}+\text{H.c.}]+i\sum_{i,n,\sigma}\delta\lambda_i(\tau)n^{i}_{fn\sigma}(\tau)\ . \tag{26}$$

The terms in $\delta\lambda_i$ are important as they ensure the constraint is enforced at each level of the approximation, as has been shown to leading order in $1/N$. The interaction determines the boson propagators

$$D_{\lambda\lambda}=\langle\delta\lambda(\mathbf{q},\omega),\delta\lambda(-\mathbf{q},-\omega)\rangle\ ,$$
$$D_{\lambda r}=\langle\delta\lambda(\mathbf{q},\omega),\delta r(-\mathbf{q},-\omega)\rangle\ , \tag{27}$$
$$D_{rr}=\langle\delta r(\mathbf{q},\omega),\delta r(-\mathbf{q},-\omega)\rangle\ .$$

Following Millis and Lee,[16] we assume that the resistivity arises from the scattering of the conduction electrons off the Bose fluctuations. We equate the scattering rate $1/\tau_\sigma$ to twice the conduction-electron lifetime 2 $\mathrm{Im}\Sigma^c_\sigma$. In general, this is not the correct procedure and we need to consider the retarded two-particle Green function. However, the fact that the f electrons are dispersionless means that the model is not Galilean invariant and we expect the calculation of the conduction-electron lifetime to give essentially the correct result. To calculate $\mathrm{Im}\Sigma^c_\sigma$, we use the standard functional-integral technique. The diagrammatic representation to first order in the boson fluctuations is shown in Fig. 1, where we see that there are three types of diagrams. By a simple extension of the results obtained previously, we obtain

$$\begin{aligned}\bar{G}^c_\sigma(\mathbf{k},\omega)=G^c_\sigma(\mathbf{k},\omega)&+\sum_n[G^{fc}_{n\sigma}(\mathbf{k},\omega)]^2\sum_{q,v}G^f_{n\sigma}(\mathbf{q},v)D_{\lambda\lambda}(\mathbf{k}+\mathbf{q},\omega+v)\\&+2G^c_\sigma(\mathbf{k},\omega)\sum_n Vh_n(\mathbf{k})G^{fc}_{n\sigma}(\mathbf{k},\omega)\sum_{q,v}G^f_{n\sigma}(\mathbf{q},v)D_{\lambda r}(\mathbf{k}+\mathbf{q},\omega+v)\\&+2[G^c_\sigma(\mathbf{k},\omega)]^2\sum_n V^2h_n^2(\mathbf{k})\sum_{q,v}G^f_{n\sigma}(\mathbf{q},v)D_{rr}(\mathbf{k}+\mathbf{q},\omega+v)\ ,\end{aligned} \tag{28}$$

where $G^f_{n\sigma}$ and G^c_σ are the Green functions for the f and conduction (c) electrons, respectively, and $G^{fc}_{n\sigma}$ is the mixed propagator $\langle f_{n\sigma};c^*_{k\sigma}\rangle$. These are all calculated using the mean-field Hamiltonian (25). $\bar{G}^c_\sigma$ is the c-electron Green function including corrections coming from the fluctuation terms. The following relation is easily shown:

$$G^{fc}_{n\sigma}(\mathbf{k},\omega)=\frac{\tilde{V}h_n(\mathbf{k})}{\omega-\varepsilon_{fn}}G^c_\sigma(\mathbf{k},\omega)\ , \tag{29}$$

and we can then identify

$$\begin{aligned}\Sigma^c_\sigma(\mathbf{k},\omega)=\sum_{n=0,1,2}\Bigg[&\frac{\tilde{V}^2h_n^2(\mathbf{k})}{(\omega-\varepsilon_{fn})^2}\sum_{\mathbf{q},v}G^f_{n\sigma}(\mathbf{q},v)D_{\lambda\lambda}(\mathbf{k}+\mathbf{q},\omega+v)+2\frac{\tilde{V}Vh_n^2(\mathbf{k})}{(\omega-\varepsilon_{fn})}\sum_{\mathbf{q},v}G^f_{n\sigma}(\mathbf{q},v)D_{\lambda r}(\mathbf{k}+\mathbf{q},\omega+v)\\&+V^2h_n^2(\mathbf{k})\sum_{\mathbf{q},v}G^f_{n\sigma}(\mathbf{q},v)D_{rr}(\mathbf{k}+\mathbf{q},\omega+v)\Bigg]\ .\end{aligned} \tag{30}$$

Taking the imaginary part, we obtain an expression involving both Fermi and Bose distribution functions corresponding to the Green functions and Boson propagators involved in (30). We then take the limit $T,\ \omega\to0$ and obtain the $(\omega^2+\pi^2T^2)$ dependence of the self-energy, which is characteristic of the Fermi-liquid behavior. The $|\mathbf{k}|$ dependence of the self-energy is small, because of the Fermi functions involved in the integrals, and we can replace $|\mathbf{k}|$ by k_F; however, the angular dependence of the self-energy on $\hat{\mathbf{k}}$ remains important through the functions $h_n(\hat{\mathbf{k}})$ of the spherical harmonics $Y_3^{M-\sigma}(\hat{\mathbf{k}})$. The imaginary part of the self-energy is, therefore, given, in the limit $T,\ \omega\to0$, by

$$\begin{aligned}\mathrm{Im}\Sigma^c_\sigma(\omega)=\sum_{n=0,1,2}\Bigg[&\frac{\tilde{V}^2h_n^2(\hat{\mathbf{k}})}{(\omega-\varepsilon_{fn})^2}\rho(E_F)\frac{\tilde{V}^2}{\varepsilon^2_{fn}}\left[\lim_{\omega\to0}\frac{\mathrm{Im}D_{\lambda\lambda}(k_F,\omega)}{\omega}\right]+2\frac{\tilde{V}Vh_n^2(\hat{\mathbf{k}})}{(\omega-\varepsilon_{fn})}\rho(E_F)\frac{\tilde{V}^2}{\varepsilon^2_{fn}}\left[\lim_{\omega\to0}\frac{\mathrm{Im}D_{\lambda r}(k_F,\omega)}{\omega}\right]\\&+V^2h_n^2(\hat{\mathbf{k}})\rho(E_F)\frac{\tilde{V}^2}{\varepsilon^2_{fn}}\left[\lim_{\omega\to0}\frac{\mathrm{Im}D_{rr}(k_F,\omega)}{\omega}\right]\Bigg](\omega^2+\pi^2T^2)\ .\end{aligned} \tag{31}$$

$\rho(E_F)$ is the bare conduction-electron density of states evaluated at the Fermi energy. In principle we need to know the full band structure to calculate the boson propagators and these will depend on direction of $\mathbf{k}$. This is complicated and instead we approximate here the boson propagators by the values calculated by an isotropic f level with a degeneracy of 2; this gives

$$\begin{aligned}\lim_{\omega\to0}\frac{\mathrm{Im}D_{\lambda\lambda}(k_F,\omega)}{\omega}&=\frac{1}{2}\ ,\\ \lim_{\omega\to0}\frac{\mathrm{Im}D_{\lambda r}(k_F,\omega)}{\omega}&=\left[\frac{\tilde{V}}{\varepsilon_{f0}}\right]\frac{1-n_f}{2V}\ ,\\ \lim_{\omega\to0}\frac{\mathrm{Im}D_{rr}(k_F,\omega)}{\omega}&=\left[\frac{\tilde{V}}{\varepsilon_{f0}}\right]^2\frac{1-n_f}{2V^2}\ ,\end{aligned} \tag{32}$$

where corrections are $O(\varepsilon_{f0}/\Delta_1,\varepsilon_{f0}/\Delta_2)$ or, in other words, the neglected terms are in T_k/Δ_1 or T_k/Δ_2. We see that, for contributions to the self-energy coming from $n_f\to1$, the contribution from diagrams involving $D_{\lambda r}$ and D_{rr} are a factor $(1-n_f)$ smaller than those involving $D_{\lambda\lambda}$ and so can be neglected in the limit $n_f\to1$. When we look at the terms from the higher-energy doublets ($n=1$ and 2), we see that the contributions from D_{rr} and $D_{\lambda r}$ are of the order $(1-n_f)\varepsilon^2_{fn}/\varepsilon^2_{f0}$ and $(1-n_f)\varepsilon_{fn}/\varepsilon_{f0}$ times that from $D_{\lambda\lambda}$, respectively. With n_f close to one and the crystal fields not too large, these terms can be neglected also.

In the opposite limit with $\Delta_1=\Delta_2=0$ and a degeneracy of the $4f$ level equal to $N=6$, we obtain a simple factor:

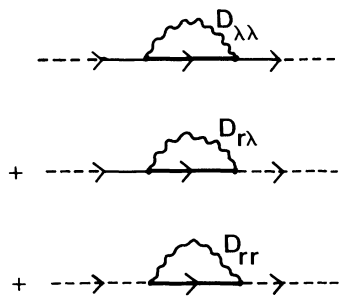

FIG. 1. Diagrammatic representation of the three types of diagrams involved in Eq. (28). The figure is drawn here for each n value. The full line (——→——) represents the Green function $G^f_{n\sigma}(\mathbf{k},\omega)$, the broken line (– – –→– – –) $G^c_\sigma(\mathbf{k},\omega)$, and the mixed line (——→– – –) $G^{cf}_{n\sigma}(\mathbf{k},\omega)$.

$$\lim_{\omega\to 0}\frac{\mathrm{Im}D_{\lambda\lambda}(k_F,\omega)}{\omega}=\frac{1}{N}\ . \tag{33}$$

We note that we could also have obtained the same result in the following way: We start from the "spin-N" model in which the conduction electrons are taken as having the same total angular momentum as the $4f$ electrons and V is taken as constant, then we calculate the scattering rate $1/\tau_{k\mu}$ within a particular spin channel, and finally we use the analogy with the one impurity problem expressed by the relation (7) between the total scattering rate $1/\tau_{\mathbf{k}\sigma}$ and the partial ones $1/\tau_{k\mu}$.

B. The low-temperature transport properties

We will now derive theoretically the transport properties at low temperatures ($T\ll T_k$), for both the case of a pure lattice and the case of an additional constant impurity scattering rate. The three transport coefficients are given by the expressions (3), (4), and (5), respectively. The relaxation time $\tau_{\mathbf{k}\sigma}$, involved in the formula (6), is equal to

$$\frac{\hbar}{\tau_{\mathbf{k}\sigma}}=2\,\mathrm{Im}\Sigma^c_\sigma(\varepsilon_{\mathbf{k}})\ , \tag{34}$$

where the imaginary part of the self-energy is given by (31).

The electrical conductivity σ_i along the principal axis i can, therefore, be written as

$$\sigma_i=\left[\frac{e\hbar k_F}{m_i}\right]^2\frac{\hbar}{v_0 c}\sum_\sigma\int\hat{k}_i^2\left[-\frac{\partial f_{\mathbf{k}}}{\partial\varepsilon_{\mathbf{k}}}\right]\frac{d\mathbf{k}}{2\,\mathrm{Im}\Sigma^c_\sigma(\varepsilon_{\mathbf{k}})}\ , \tag{35}$$

with the same notations as in the previous section. $\hat{k}_i=\mathbf{k}_i/|\mathbf{k}|$ and we write $\hat{k}_z^2=x^2$, $\hat{k}_x^2=(1-x^2)\cos^2\phi$, and $\hat{k}_y^2=(1-x^2)\sin^2\phi$, with $x=\cos\theta$.

Thus, inserting (31) into (35) yields

$$\sigma_i=\left[\frac{e\hbar k_F}{m_i}\right]^2\frac{\hbar}{v_0 c}\frac{CB_i}{12T^2}\ , \tag{36}$$

where

$$\frac{1}{C}=\lim_{\omega\to 0}\frac{\mathrm{Im}D_{\lambda\lambda}(k_F,\omega)}{\omega} \tag{37}$$

and

$$B_i=\frac{1}{2\pi}\int_0^{2\pi}\int_0^1 d\phi\,dx\frac{\hat{k}_i^2}{\sum_{n=0}^{2}h_n^2(\hat{k}_i^2)\rho(E_F)\left[\frac{\tilde{V}}{\varepsilon_{fn}}\right]^4}\ . \tag{38}$$

We have used here the fact that

$$\int_{-\infty}^{+\infty}d\varepsilon\left[-\frac{\partial f(\varepsilon)}{\partial\varepsilon}\right]\frac{1}{\varepsilon^2+\pi^2T^2}=\frac{1}{12T^2}\ , \tag{39}$$

which can be shown by usual integration in the complex plane after expanding the Fermi function according to its imaginary poles.

Thus, the resistivity $\rho_i=1/\sigma_i$ along the i axis is given by

$$\rho_i=\rho_U\frac{12T^2\rho(E_F)^2}{CB_i}\ , \tag{40}$$

where the constant value ρ_U is given by

$$\rho_U=\frac{m_i^2 v_0 c}{e^2\hbar^3 k_F^2\rho(E_F)^2}\ . \tag{41}$$

We note that if we average over direction the denominator of (38), and set $h_n(\mathbf{k})=\langle h_n(\mathbf{k})\rangle$, the resistivity is given by

$$\rho=\frac{36}{C}\rho_U\rho(E_F)^2T^2\sum_n\left[\frac{\tilde{V}}{\varepsilon_{fn}}\right]^4\ , \tag{42}$$

which can be rewritten

$$\rho=\frac{9}{C}\rho_U T^2\sum_n\left[\frac{n_{fn}}{\varepsilon_{fn}}\right]^2\ , \tag{43}$$

where

$$n_{fn}=\frac{2\rho(E_F)\tilde{V}^2}{\varepsilon_{fn}}$$

denotes the average occupation of the nth doublet. Each doublet gives a contribution to the resistivity of the form T^2 scaled by the inverse of the appropriate energy scale squared. The factors in n_{fn} reflect the fact that, if the doublet is unoccupied, there is no scattering. In the limit $\Delta\to 0$ we obtain $n_{fn}=\frac{1}{3}$, $\varepsilon_{fn}=\varepsilon_f$, $C=6$, and

$$\rho=\frac{\rho_U}{2}\left[\frac{T}{\varepsilon_f}\right]^2\ , \tag{44}$$

while for $\Delta\to\infty$ we obtain $n_{f0}=1$, $n_{f1}=n_{f2}=0$, $C=2$, and

$$\rho=\frac{9\rho_U}{2}\left[\frac{T}{\varepsilon_{f0}}\right]^2\ . \tag{45}$$

We now look at the anisotropy. We consider first the simplest case where the crystal-field states are pure M states. Here the dependence on ϕ drops out and

$$[h_{\pm 1/2}(x)]^2=\tfrac{3}{4}(1-2x^2+5x^4)\ ,$$
$$[h_{\pm 3/2}(x)]^2=\tfrac{3}{8}(1+14x^2-15x^4)\ , \quad (46)$$
$$[h_{\pm 5/2}(x)]^2=\tfrac{15}{8}(1-2x^2+x^4)\ .$$

ρ_x is now equal to ρ_y, which remains true when we generalize to the case where the crystal-field levels are given by $|\pm\frac{1}{2}\rangle$ and linear combinations of $|\pm\frac{3}{2}\rangle$ and $|\mp\frac{5}{2}\rangle$. These crystal-field levels are relevant in crystals of hexagonal and tetragonal symmetry.

For large crystal fields we may be tempted to include only the ground state in this expression. In this case we find that while the values of B_i are finite for a ground state $\pm\frac{1}{2}$, B_z diverges as $\log x$ for a ground state $\pm\frac{3}{2}$, and B_z and $B_{x,y}$ diverge as x^{-2} and $\log x$, respectively, for a ground state $\pm\frac{5}{2}$.[34] It is therefore seen to be important to include all the levels. Nonetheless, as Δ becomes large, the anisotropy can become very large especially when the ground state is $\pm\frac{5}{2}$. Two factors tend to reduce this. First we note that, even when the ground state is nominally $|\pm\frac{5}{2}\rangle$, adding in a small admixture of $|\pm\frac{3}{2}\rangle$ will do a lot to suppress the tendency to divergence. Adding in an admixture of $|\pm\frac{1}{2}\rangle$ as for orthorhombic crystals will suppress all tendency to divergence.

The other factor that will tend to reduce the anisotropy is the presence of impurity scattering. In general we can write $\tau_\sigma^{-1}=\tau_{0\sigma}^{-1}+\tau_{e\sigma}^{-1}$, where $\tau_{0\sigma}$ is due to impurity scattering and $\tau_{e\sigma}$ due to electron-electron scattering. In this section we assume that $\tau_{0\sigma}$ arises purely from disorder on the c-electron sites.[16] In this case, $\tau_{0\sigma}$ is isotropic and temperature independent. For small enough temperatures, we can always expand $\tau_\sigma\sim\tau_{0\sigma}-2\tau_{0\sigma}^2\,\mathrm{Im}\Sigma_c^\sigma$. Substituting into the equation for σ_i, we now have

$$\rho_i=\rho_0+\rho_U\frac{6\pi}{C}T^2\rho(E_F)^2 \times\int_0^{2\pi}\int_0^1 dx\,d\phi\,\hat{k}_i^2\sum_n\left[\frac{\tilde{V}}{\varepsilon_{fn}}\right]^4 h_n(\hat{\mathbf{k}})^2\ , \quad (47)$$

where ρ_0 is the constant residual resistivity arising from impurity scattering $\tau_{0\sigma}$. In the limit $\Delta\to 0$ we obtain

$$\rho=\rho_0+\frac{2\pi^2\rho_U}{9}\left[\frac{T}{\varepsilon_f}\right]^2\ ,$$

while for large Δ if we replace $h_n(\hat{\mathbf{k}})$ by its average, we obtain

$$\rho=\rho_0+2\pi^2\rho_U\left[\frac{T}{\varepsilon_{f0}}\right]^2$$

When we include the anisotropy we now find integrals we can do analytically and we obtain different results for the anisotropy of A. In particular all tendency for divergence is completely suppressed and the anisotropy is smaller. For example, we can compute numerically the coefficients A_i in the simple case of pure M states with large crystal-field splittings. The integration is quite obvious in this case, since A_i is proportional to the angular integration of $\hat{k}_i^2 h_n(\hat{\mathbf{k}})^2$. Thus, we obtain the following results for the ratio $A_\perp/A_\parallel$ of the A coefficients determined along the x or y directions ($A_\perp$) and along the z direction ($A_\parallel$):

(i) For a $\pm\frac{1}{2}$ ground state, $A_\perp/A_\parallel=0.53$.

(ii) For a $\pm\frac{3}{2}$ ground state, $A_\perp/A_\parallel=0.85$.

(iii) For a $\pm\frac{5}{2}$ ground state, $A_\perp/A_\parallel=3$. These results will be used in Sec. V when comparing our results to experiment.

Let us now consider the other transport properties, i.e., the thermoelectric power S, the thermal conductivity K, and the Lorenz number L. K and S are, respectively, given by expressions (4) and (5), while L is given by

$$\frac{L}{L_0}=\frac{3}{(\pi T)^2}\left[\frac{K_2}{K_0}-\left[\frac{K_1}{K_0}\right]^2\right]\ , \quad (48)$$

as a function of the integrals K_n given by (6) and of the Sommerfeld value

$$L_0=\frac{\pi^2 k_B^2}{3e^2}=2.45\times 10^{-8}\ \mathrm{W\,\Omega\,K^{-2}}\ .$$

The lowest-order contribution to the thermoelectric power S comes from the odd part of τ coming from the factors $1/(\omega-\varepsilon_{fn})^2$ in Σ_σ^c. In the case of a pure lattice, S is easily seen to be linear in T, while in the case where impurity scattering is important, S is in T^3. In both cases, L is constant.

In the case of a pure lattice, the thermoelectric power S_i along the principal axis i is given by

$$\frac{eS_i}{T}=2(12-\pi^2)\frac{C_i}{B_i}\ , \quad (49)$$

where

$$C_i=\frac{1}{2\pi}\int_0^{2\pi}\int_0^1 d\phi\,dx\,\hat{k}_i^2(x,\phi)\left[\frac{\sum_n h_n^2(\tilde{V}^4/\varepsilon_{fn}^5)}{\left[\sum_n h_n^2(\tilde{V}^4/\varepsilon_{fn}^4)\right]^2}\right]\ . \quad (50)$$

We have used here the fact that

$$\int d\varepsilon\left[-\frac{\partial f(\varepsilon)}{\partial\varepsilon}\right]\frac{\varepsilon^2}{\varepsilon^2+\pi^2T^2}=1-\frac{\pi^2}{12}\ . \quad (51)$$

It is easily seen that the anisotropy of S vanishes in the two limits $\Delta=0$ and $\Delta\to\infty$ and we obtain the result

$$S=\frac{2(12-\pi^2)}{e}\frac{T}{T_k}\ , \quad (52)$$

where $T_k=\varepsilon_f$ or ε_{f0}, respectively. For finite values of Δ, S is anisotropic. The anisotropy of the linear T term is, however, small.

If we now include impurity scattering we obtain

$$\frac{eS_i}{T}\cong 2\pi^3T^3\tau_0\rho(E_F)^2\int_0^{2\pi}\int_0^1 dx\,d\phi\,\hat{k}_i^2\sum_n h_n^2\frac{\tilde{V}^4}{\varepsilon_{fn}^5}\ . \quad (53)$$

The anisotropy of the term in T^3 is approximately the same as that for the T^2 term in the resistivity [Eq. (47)].

In contrast L/L_0 is isotropic for all Δ with the value $36/\pi^2-3$ when electron scattering dominates and 1 when impurity scattering is important. We can consider also the thermal conductivity, which is given by (4) and can be written as

$$K=\frac{\pi T K_0}{3}\frac{L}{L_0} . \tag{54}$$

For a pure lattice, this diverges as $1/T$ and has the same anisotropy as $1/\rho_i$. The addition of impurities suppresses the divergence and instead K goes to 0 linearly with T, but there is no longer any anisotropy in this case.

IV. ANISOTROPY OF THE RESIDUAL RESISTIVITY AND ITS RELATION WITH THE T^2-LAW COEFFICIENT

In this section, we reexamine the problem of the residual resistivity ρ_0 and of its anisotropy. Experimentally, ρ_0 has been found to be large and anisotropic in some single-crystal cerium Kondo compounds. Moreover, it has been noted, in a few cases, that there appears to be a relation between ρ_0 and the coefficient A of the T^2 law of the low-temperature resistivity. For example, in $CeAl_3$ single crystals,[35] both ρ_0 and A are anisotropic, with $\rho_{0\perp}=9.9$ $\mu\Omega$ cm, $\rho_{0\parallel}=14.5$ $\mu\Omega$ cm, and $A_\perp=13.3$ $\mu\Omega\,\mathrm{cm/K^2}$, $A_\parallel=4.6$ $\mu\Omega\,\mathrm{cm/K^2}$. The same type of relation yielding an increase of A with decreasing ρ_0 values has been also observed in $CeRu_2Si_2$ single crystals, but the situation is more controversial in $CeCu_6$ single crystals.[21,22,25] However, it has been pointed out that the relation between an increase of A and a decrease of ρ_0 in an approximately linear fashion can be interpreted as a temperature-dependent impurity contribution.[35] These properties strongly suggest that disorder on the f sites is also playing a role and a possible interpretation is that ρ_0 arises from Kondo hole scattering.[36] It is, therefore, of interest to consider an alloy system in which a fraction $(1-c)$ of Ce ions are removed. We start by considering the zero-temperature resistivity obtained from Kondo impurity scattering and go on to consider the alloy system using a simple formula. We use this to calculate the anisotropy of ρ_0 and to consider the effect this has on both the magnitude and anisotropy of A.

The calculation of ρ_0 for a Kondo impurity is particularly simple as it arises from the mean-field solution. We use the same Hamiltonian as before in (20) but now the sum over i is restricted to a single site. Using the slave-boson method we obtain for the mean-field f-impurity Green function

$$G^f_{n\sigma}(\omega)=\frac{1}{\omega-\varepsilon_{fn}-i\tilde{\Gamma}} , \tag{55}$$

where $\tilde{\Gamma}=(1-n_f)\rho(E_F)V^2\pi$.

The effective f doublet energy, ε_{fn}, for the impurity is taken as equal to that for the lattice. The conduction-electron Green function $G^c_\sigma(\mathbf{k},\omega)$ is given in terms of $G^f_{n\sigma}(\omega)$ by

$$G^c_\sigma(\mathbf{k},\omega)=\frac{1}{\omega-\varepsilon_{\mathbf{k}}}+\sum_n \frac{\tilde{V}^2h_n^2}{(\omega-\varepsilon_{\mathbf{k}})^2}G^f_{n\sigma}(\omega) . \tag{56}$$

From this, the conduction-electron self-energy is easily found to be

$$\Sigma^c_\sigma(\omega)=\sum_n \tilde{V}^2h_n^2G^f_{n\sigma}(\omega) ,$$

giving

$$\mathrm{Im}\Sigma^c_\sigma=\sum_n \tilde{V}^2h_n^2\frac{\tilde{\Gamma}}{(\omega-\varepsilon_{fn})^2+\tilde{\Gamma}^2} . \tag{57}$$

If we average over direction and replace $h_n(\mathbf{k})$ by $\langle h_n(\mathbf{k})\rangle$ we can evaluate ρ at $T=0$ to give

$$\rho_0=\rho_U\frac{3}{\pi}\sum_n\frac{\tilde{\Gamma}^2}{\varepsilon_{fn}^2+\tilde{\Gamma}^2} , \tag{58}$$

with ρ_U given by (41).

Taking now the anisotropy into account we find $\rho_{0i}=\rho_U/(\pi B_{0i})$, where

$$B_{0i}=\frac{1}{2\pi}\int_0^{2\pi}\int_0^1 d\phi\,dx\frac{\hat{k}_i^2}{\sum_n h_n^2\tilde{\Gamma}^2/(\varepsilon_{fn}^2+\tilde{\Gamma}^2)} . \tag{59}$$

In general the anisotropy is in the same sense as for A calculated for the pure lattice but the presence of the terms in $\tilde{\Gamma}^2$, which are independent of n, tends to give a much smaller anisotropy for given crystal fields.

To look at the term in T^2 we need to include the term in the self-energy coming from the boson fluctuations. If we do this we obtain a term in $(\omega^2+\pi^2T^2)$ very similar to that found for the lattice. Using this it is easily seen that ρ decreases at $(T/T_k)^2$.

What we are really interested in here is the alloy system where we assume a concentration c of Ce ions. To treat this case we follow the procedure of Cox and Grewe[17] based on the average-T-matrix approximation. The method starts from the self-energy for an impurity, then explicitly subtracts off the elastic scattering when we go over to the periodic case. It is assumed that the conduction-electron self-energy for the lattice is related to the impurity f-electron Green function in the following way:

$$\Sigma^c_\sigma(\omega)=\sum_n \tilde{V}^2h_n^2[(G^f_{n\sigma})^{-1}+i\tilde{\Gamma}]^{-1} . \tag{60}$$

We shall take the T- and ω-dependent contribution to the self-energy as being the same for the impurity and the lattice. Then, using (55) together with (31) we obtain

$$\mathrm{Im}\Sigma^c_\sigma=\sum_n \tilde{V}^2h_n^2\frac{(\omega^2+\pi^2T^2)\rho(E_F)\tilde{V}^2/(C\varepsilon_{fn}^2)}{(\omega-\varepsilon_{fn})^2+[(\omega^2+\pi^2T^2)\rho(E_F)\tilde{V}^2/(C\varepsilon_{fn}^2)]^2} . \tag{61}$$

This differs from (31) by the term in $(\omega^2+\pi^2T^2)^2$ appearing in the denominator. We note that this can be obtained by self consistently taking account of the f-electron self-energy in calculating G^{fc}, i.e., we replace $G^{fc}_{n\sigma}$ by $\tilde{V}^2h_n^2/(\omega-\varepsilon_{fn}-\Sigma^f_{n\sigma})$.

We can now extend to the alloy. Following again Cox and Grewe,[17] we assume that the conduction-electron self-energy is proportional to the number of Ce ions and that the cancellation of the elastic-scattering term is incomplete. We then have

$$\Sigma^c_\sigma = c\sum_n \tilde{V}^2h_n^2\{[G^f_{n\sigma}(\omega)]^{-1}+ic\tilde{\Gamma}\}^{-1}\ , \tag{62}$$

where c is the concentration of Ce ions. This gives

$$\mathrm{Im}\Sigma^c_\sigma = c\sum_n \tilde{V}^2h_n^2\frac{(1-c)\tilde{\Gamma}+(\omega^2+\pi^2T^2)\rho(E_F)\tilde{V}^2/(C\varepsilon^2_{fn})}{(\omega-\varepsilon_{fn})^2+[(1-c)\tilde{\Gamma}+(\omega^2+\pi^2T^2)\rho(E_F)\tilde{V}^2/(C\varepsilon^2_{fn})]^2} \tag{63}$$

If we average over direction, then at $T=0$ we obtain

$$\rho_A = \frac{3}{\pi}\rho_U c(1-c)\sum_n \frac{\tilde{\Gamma}^2}{\varepsilon^2_{fn}+(1-c)^2\tilde{\Gamma}^2}\ . \tag{64}$$

We note that we get approximately the Nordheim factor of $c(1-c)$, though the c dependence of the denominator prevents this from being followed exactly.

The anisotropy can also be included. We now obtain

$$\rho_{Ai} = \rho_U c(1-c)/(\pi B_{Ai})\ , \tag{65}$$

where

$$B_{Ai} = \frac{1}{2\pi}\int_0^{2\pi}\int_0^1 d\phi\,dx \frac{\hat{k}_i^2}{\sum_n h_n^2\tilde{\Gamma}^2/[\varepsilon^2_{fn}+(1-c)^2\tilde{\Gamma}^2]}\ . \tag{66}$$

This differs from B_{0i} for a single impurity by the factors $(1-c)$ in the denominator. For c close to 1, the anisotropy is greater than that for a single impurity. It is similar to that for the pure lattice, though it still tends to be smaller as the terms for the higher-lying doublets fall off only as $1/\Delta^2$ rather than $1/\Delta^4$. The inclusion of a certain amount of disorder on the noncerium sites will tend to reduce the anisotropy.

We can now calculate the T^2 term. We look first at the case where we average over direction and take the limit $c\sim 1$. We obtain the following result:

$$\rho=\rho_A+(2\rho_U\pi^2-\rho_A\frac{\pi^2}{3})\frac{T^2}{(C\varepsilon_f)^2}\ , \tag{67}$$

where, for $\Delta=0$, ε_f is the f-level energy and $C=6$ and, for large Δ, ε_f is the energy of the ground-state doublet and $C=2$. We see that we do indeed obtain a factor A which decreases linearly with increasing ρ_A.

We can also use our result to reconsider the anisotropy of A. Expanding in T^2 and ω^2 we find

$$\rho_i=\rho_{Ai}+\rho_U\frac{2\pi}{3C}T^2\rho(E_F)^2\frac{1}{B_i^2}\int_0^{2\pi}\int_0^1 d\phi\,dx\frac{\hat{k}_i^2\sum_n h_n^2/\varepsilon^4_{fn}}{(\sum_n h_n^2/\varepsilon^2_{fn})^2}, \tag{68}$$

where we have dropped the term in $\rho_{Ai}T^2$ because this term in ρ_{Ai} is proportional to c and is certainly smaller here than the term in ρ_U, so that it can be neglected when we look at the anisotropy of the T^2 term. The anisotropy of A is, therefore, in the same sense as for the pure lattice but with a somewhat different, usually smaller, magnitude.

We note finally that the result for the decrease in A is very similar to that found in the phenomenological model proposed by Fetisov and Khomskii.[37] We would also expect the results for the anisotropy to be the same in this model.

V. RESULTS AND DISCUSSION

A. Theoretical results

Thus, we have presented here a full theoretical description for the anisotropy of transport properties, by treating successively the high-temperature regime ($T\gg T_k$) and the low-temperature one without or with impurity scattering. In particular, we have found a linear relation between the increase in the value of A, the coefficient of the T^2 term, and the decrease of the residual resistivity ρ_0.

Theoretical plots of the transport properties have been previously derived for the high-temperature domain and a good agreement has been obtained for the cases of tetragonal $CePt_2Si_2$ (Refs. 18 and 38) and orthorhombic $CeCu_6$ (Ref. 26) single crystals; in the case of $CePt_2Si_2$, we have taken a ratio m_z/m_x of the effective masses typically of order 1.5 in order to have a reasonable fit to the experimental curves.[18,38] Up to now, there are no available data on ytterbium Kondo compounds showing an anisotropy, which could be accounted for by the theoretical results presented in Sec. II.

Let us discuss now the theoretical results obtained at low temperatures for the case of hexagonal or tetragonal symmetry. As an example, we take here $\Delta_2=2\Delta_1$ and we calculate the ratio $A_\perp/A_\parallel$ versus the ratio Δ_1/T_k for different crystal-field schemes. Thus we show the results for a pure lattice with no impurity scattering in Fig. 2 and for an imperfect lattice when a finite amount of impurity scattering is included in Fig. 3. The broken line is for crystal field levels:

$$|0\rangle=|\pm\tfrac{1}{2}\rangle,\quad |1\rangle=|\pm\tfrac{3}{2}\rangle,\quad |2\rangle=|\pm\tfrac{5}{2}\rangle\ . \tag{69}$$

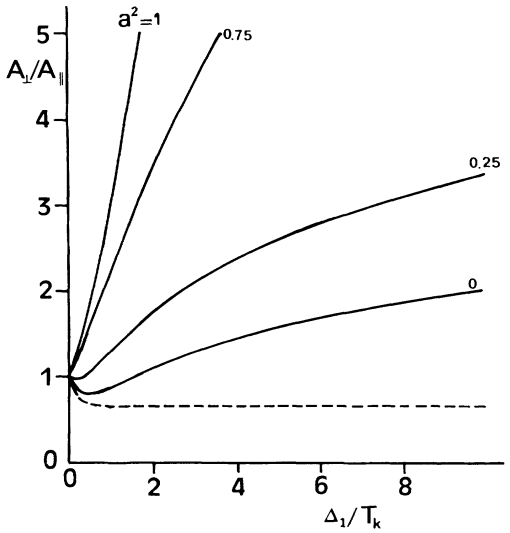

FIG. 2. Plot vs Δ_1/T_k with $\Delta_2=2\Delta_1$ for the theoretical values of $A_\perp/A_\parallel$ computed for a pure lattice and for different crystal-field schemes: the broken line corresponds to the crystal-field scheme given by (69), while the full lines correspond to those given by (70) with different values of a^2.

Here $A_\perp < A_\parallel$ with the anisotropy quickly reaching a constant value of $A_\perp/A_\parallel=0.67$ in the case of a pure lattice and $A_\perp/A_\parallel=0.53$ in the case of an imperfect one.

The other curves of the two figures have been derived for a crystal-field scheme:

$$|0\rangle=a|\pm\tfrac{5}{2}\rangle+b|\mp\tfrac{3}{2}\rangle\ ,$$
$$|1\rangle=|\pm\tfrac{1}{2}\rangle\ , \qquad (70)$$
$$|2\rangle=b|\pm\tfrac{5}{2}\rangle-a|\mp\tfrac{3}{2}\rangle\ ,$$

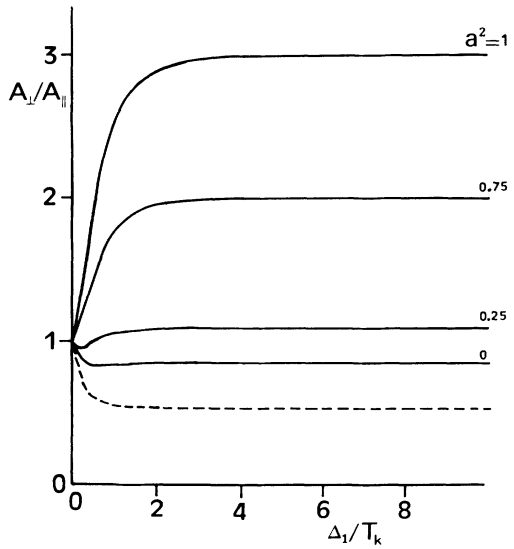

FIG. 3. Plot vs Δ_1/T_k with $\Delta_2=2\Delta_1$ for theoretical values of $A_\perp/A_\parallel$ computed for an imperfect lattice with a constant isotropic impurity scattering and for different crystal-field schemes: the broken line corresponds to the crystal-field scheme given by (69), while the full lines correspond to those given by (70) with different values of a^2.

TABLE I. Experimental values of the parameters for the crystal-field levels of several compounds: The coefficients a and b refer to the crystal-field scheme given by (70); T_k, Δ_1, and Δ_2 (expressed in K) are the Kondo temperature and the two crystal-field splittings, respectively.

Compound	a	b	T_k	Δ_1/T_k	Δ_2/T_k
$CeCu_2Si_2$	0.83	0.56	10	14	36
$CeRu_2Si_2$	0.96	0.28	19	12	53
$CeAl_3$	0.24	0.97	3	20	30
$CeSi_{1.86}$	0.45	0.89	20	17	14

with different values of a. In Fig. 2, for Δ_1 not too small, $A_\perp > A_\parallel$ and, as Δ_1 becomes large, the anisotropy can be very large especially when there is an appreciable component of $|\pm\frac{5}{2}\rangle$ in the ground state. On the other hand, when impurity scattering is taken into account, the anisotropy is in general much smaller and the ratio $A_\perp/A_\parallel$ saturates for large Δ_1 values. Thus, when the ground state is $|\pm\frac{5}{2}\rangle$ or close to it, we predict here $A_\perp > A_\parallel$, while, when the ground state is $|\pm\frac{1}{2}\rangle$ or $|\pm\frac{3}{2}\rangle$ with an important impurity scattering, the present theoretical model yields a reversed sense of anisotropy with $A_\perp < A_\parallel$. The limiting values of $A_\perp/A_\parallel$ for very large Δ_1 values have been already computed in Sec. III B by use of expression (47).

Only a few cerium Kondo compounds have been studied in single crystals, but generally their crystal-field levels are known. Tetragonal $CePt_2Si_2$ has crystal-field levels given by (69) with $\Delta_1=80$ K and $\Delta_2=230$ K. The other compounds, $CeCu_2Si_2$, $CeRu_2Si_2$, $CeAl_3$, and $CeSi_{1.86}$ have crystal-field levels given (70) and Table I gives the corresponding a and b coefficients, as well as an estimate of T_k, Δ_1, and Δ_2. Finally, orthorhombic $CeCu_6$ has two excited doublets lying at 87 and 210 K above the ground state and all the corresponding wave functions are linear combinations of the three $\pm\frac{1}{2}$, $\pm\frac{3}{2}$, $\pm\frac{5}{2}$ wave functions.[41,42]

B. Comparison with experiment

We discuss here our numerical results in the light of experimental data. We note that the comparison with experiment is complicated by several features. First of all, there is not much available data in single crystals, especially at very low temperatures. Furthermore, at very high temperatures, i.e., for temperatures much larger than the overall splitting, the experimental resistivity can still have an important anisotropy, as, for example, in the case of $CePt_2Si_2$, while the mechanism for the anisotropy in our model is not expected to be very effective at very high temperatures, as shown in Sec. II or previously in Ref. 18. This suggests that there are other mechanisms for the anisotropy which could arise from the anisotropy of the Fermi surface and also from the anisotropy of the mixing parameter which has been considered by Zhang and Levy.[34] Thus, in order to improve the description of the anisotropic transport properties, we use the phenomenological assumption of taking the effective electron masses m_x, m_y, m_z to be different in the three directions

x,y,z. Although this is clearly oversimplified, we have previously obtained a good fit to the transport properties of $CePt_2Si_2$ by taking a ratio m_z/m_x of order 1.5.[18,38] On the contrary, the fit of the exerimental data can be obtained in $CeCu_6$ by taking an isotropic effective mass $m_x=m_y=m_z$.[26] Finally, there is the problem of accounting for impurity scattering at low temperatures. The results we find depend sensitively on the assumptions made and the origin of ρ_0 is not well established. For the thermopower, there is not much experimental data and what data there is does not distinguish between a clear T or T^3 behavior at very low temperatures. Furthermore, the competition between positive and negative peaks observed experimentally cannot be accounted for within our model, as shown in the example of $CePt_2Si_2$.[18] Similarly there is not much data for the thermal conductivity.

Let us consider now in detail the available resistivity data in cerium Kondo compounds. Tables II and III summarize, therefore, some experimental and theoretical results on the resistivity in single crystals. Table II gives the experimental anisotropy of the residual resistivity ρ_0, of the coefficient A of the low-temperature T^2 law and of the resistivity at low ($T<T_k$) and high ($T>T_k$) temperatures. Table III gives the theoretically deduced values of $\rho_{0\perp}/\rho_{0\parallel}$ calculated on the assumption that the anisotropy is due to Kondo hole scattering and of $A_\perp/A_\parallel$ calculated for a pure lattice, then for a lattice plus isotropic impurity scattering, and finally for a lattice plus Kondo-like scattering.

We explain now these calculations in the different specific examples. We look first at tetragonal $CePt_2Si_2$, which has crystal-field levels given by (69) and $\Delta_1=1.6T_k$ and $\Delta_2=4.6T_k$, if we take the large value $T_k=50$ K experimentally deduced for the Kondo temperature.[18] The experimental anisotropy $\rho_\parallel/\rho_\perp$ is roughly 4 at low temperatures and 2 at high temperatures. Our theoretical low-temperature anisotropy is equal to 1.5–1.8, depending on our assumption for the impurity scattering. Using the value of $m_\parallel/m_\perp$ of order 1.5 estimated from the high-temperature fit of the transport properties[18,38] gives a theoretical anisotropy of 3–4 at low temperatures, in good agreement with experiment. Thus, our model explains the increase of the anisotropy $\rho_\parallel/\rho_\perp$ by a factor of 2 as one goes from high to low temperatures. There is not, however, any clear evidence for a T^2 behavior.

We look then at $CeAl_3$. The resistivity has an anisotropy $\rho_\parallel/\rho_\perp$ of order $\frac{1}{3}$ at high temperatures, above roughly 10 K.[35] At lower temperatures, $\rho_\parallel/\rho_\perp$ increases with decreasing temperature and becomes larger than 1 below 0.6 K; finally, the ratio of the residual resistivity ρ_0 is $\rho_{0\parallel}/\rho_{0\perp}=1.46$. Below 0.35 K, the resistivity follows an anisotropic T^2 law with a ratio $A_\parallel/A_\perp=0.35$. The value of the coefficient A decreases linearly with increasing ρ_0. At first sight, the experimental value for $A_\parallel/A_\perp$ appears to be consistent with our result for the pure lattice. However, it would then be difficult to account for the anisotropy at very high temperatures and the large values of ρ_0. Instead we renormalize our results by the high-temperature anisotropy as we have done for $CePt_2Si_2$.[18] Here, we take a ratio $m_\parallel/m_\perp$ of order $1/\sqrt{3}$, although it is difficult to justify taking a ratio much smaller than 1 in $CeAl_3$ and much larger in $CePt_2Si_2$. The value $A_\parallel/A_\perp=0.37$ is then found when isotropic impurity scattering is included. This is very close to the experimental value of 0.35. We still need to account for the anisotropy of ρ_0 and for the fact that A decreases with increasing ρ_0. This may seem to imply that ρ_0 arises from Kondo hole scattering. This, however, would give a large anisotropy for ρ_0 in the opposite sense to that observed and would give a value $A_\parallel/A_\perp=0.18$, which is too small. The situation could be improved by assuming ρ_0 arises from a mixture of isotropic and Kondo hole scattering.

We consider next $CeCu_2Si_2$. Here both ρ_0 and the high-temperature limit are isotropic, implying a spherical Fermi surface. For most of the samples $\rho_\parallel<\rho_\perp$ with an anisotropy up to roughly 2.[20,25] This is consistent with our result including isotropic impurity scattering.

The electrical resistivity of single-crystal tetragonal $CeRu_2Si_2$ compound has been recently measured.[7,39] The measured anisotropy $\rho_{0\perp}/\rho_{0\parallel}$ of the residual resistivity is of order 2, while the anisotropy $A_\perp/A_\parallel$ of the T^2-law coefficient is smaller and close to 1.[39] Our theoretical model predicts a very large anisotropy with $\rho_\perp \gg \rho_\parallel$, which in fact is not observed. The anisotropy of ρ_0 is in the correct sense for Kondo hole scattering, but the anisotropy for A is in the opposite sense. Thus, we cannot explain the anisotropy of $CeRu_2Si_2$ and similarly, we cannot account for the anisotropy observed in $CeSi_{1.86}$.[40]

Finally, we consider $CeCu_6$, which has an orthorhombic structure. Here the resistivity and the thermoelectric power are different along all three directions. The resis-

TABLE II. Experimental values for the anisotropy of the resistivity measured perpendicular to the c axis ($\perp$) and parallel to it ($\parallel$): ρ_0 is the residual resistivity, A is the coefficient of the T^2 law observed at low temperatures; (i) corresponds to the low-temperature ($T<T_k$) and (ii) to the high-temperature values. Blanks indicate that the data are not available.

Compound	$\rho_{0\perp}/\rho_{0\parallel}$	$A_\perp/A_\parallel$	$\rho_\perp/\rho_\parallel^{(i)}$	$\rho_\perp/\rho_\parallel^{(ii)}$
$CePt_2Si_2$			0.25	0.5
$CeCu_2Si_2$	1.0		~2	1.0
$CeRu_2Si_2$	~4	~0.7		~1.6
$CeAl_3$	0.7	2.5	3.0	3.0
$CeSi_{1.86}$	~0.6		~0.39	>1

TABLE III. Theoretical values for the anisotropy of the resistivity at low temperatures, perpendicular to the c axis ($\perp$) and parallel to it ($\parallel$): $\rho_{0\perp}/\rho_{0\parallel}$ is calculated on the assumption that the anisotropy is due to Kondo hole scattering. Three values are given for $A_\perp/A_\parallel$ calculated for (i) a pure lattice, (ii) an imperfect lattice with an isotropic impurity scattering, and (iii) an imperfect lattice with Kondo-like scattering.

Compound	$\rho_{0\perp}/\rho_{0\parallel}$	$A_\perp/A_\parallel^{(i)}$	$A_\perp/A_\parallel^{(ii)}$	$A_\perp/A_\parallel^{(iii)}$
$CePt_2Si_2$	0.66	0.65	0.54	0.64
$CeCu_2Si_2$	3.8	8.17	1.83	4.8
$CeRu_2Si_2$	5.8	17.10	2.61	12.86
$CeAl_3$	1.58	2.6	0.90	1.81
$CeSi_{1.86}$	1.99	3.67	1.04	2.31

TABLE IV. Different sets of experimental data for $CeCu_6$ showing the relative anisotropy along the three directions, according to Refs. 21, 22, and 25: ρ_0 is the residual resistivity at $T=0$, A is the coefficient of the T^2 term, B the coefficient of the T term, and the last columns correspond to the resistivity anisotropy at high temperatures.

Reference	ρ_{0x}	ρ_{0y}	ρ_{0z}	A_x	A_y	A_z	B_x	B_y	B_z	ρ_x	ρ_y	ρ_z
21	1	0.61	0.73	1	0.52	1.49				1	1	1
22	1	0.53	0.59				1	0.37	0.47	1	1	0.8
25				1	0.29	0.54				1	1	0.8

tivity has been measured in $CeCu_6$ single crystals by three different authors[21,22,25] and we report the main experimental results in Table IV, i.e., the anisotropies of the residual resistivity ρ_0, of the T^2 term, of the T term following the T^2 term, and finally of the high-temperature resistivity. The thermoelectric power has also been measured in $CeCu_6$ single crystals and presents an isotropic and almost linear behavior at low temperatures, followed by three positive peaks around 50 K and by three different decreases at high temperatures.

In order to fit the anisotropy of the transport properties of $CeCu_6$, we use the wave functions of the doublets, which are given by

$$|\Psi_n\rangle = \pm a_n|\pm\tfrac{5}{2}\rangle \pm b_n|\pm\tfrac{1}{2}\rangle \pm c_n|\mp\tfrac{3}{2}\rangle \ , \tag{71}$$

where $n=0$ corresponds to the ground state and $n=1$ and 2 to the two excited states. The results are, however, very sensitive to the values and signs of the coefficients a_n, b_n, and c_n. Two possible wave functions have been suggested, both calculated from a high-temperature fit to the magnetic susceptibility χ.[41,42] We have already used the wave function given in Ref. 41, as well as the two splittings $\Delta_1=87$ K and $\Delta_2=210$ K and an isotropic effective mass $m_x=m_y=m_z=1.5$ atomic units, in order to derive theoretical curves for both the electrical resistivity and the thermopower, as previously shown in Ref. 26. We have obtained a reasonable agreement with experiment in $CeCu_6$, in particular the three positive peaks of the thermopower occurring around 50 K.[22]

Let us now compare our model to the low-temperature experimental results on the resistivity. Table V yields the coefficients a_n, b_n, c_n of the two wave functions of Refs. 41 and 42. However, the high-temperature fit of χ used to derive them breaks down as $T\to 0$ and calculations using the slave-boson technique at $T=0$ show that neither wave function gives the observed experimental anisotropy in χ which is given by $\chi_x:\chi_y:\chi_z \sim 1:0.5:3$, i.e., $\chi_y/\chi_x=0.5$ and $\chi_z/\chi_x=3$. We propose a third wave function, with the same numerical factors as in Ref. 42 but with a change of sign. The crystal-field splitting is sufficiently large, so only the ground state is important in the low-temperature regime and moreover the wave function corresponding to the ground state contains a sizable amount of $\pm\frac{1}{2}$ states in $CeCu_6$. It results that the anisotropy of the residual resistivity calculated on the assumption that the anisotropy is due to Kondo hole scattering, the anisotropy of the T^2-coefficient A for a pure lattice, and finally the anisotropy of A for an imperfect lattice with Kondo-like scattering are approximately equal to each other. This point has been already observed in Table III for $CePt_2Si_2$, which has a $\pm\frac{1}{2}$ ground state and a large crystal-field splitting and not for the other cerium compounds, which do not contain any $\pm\frac{1}{2}$ contribution to the ground-state wave function. On the other hand, Table V gives the theoretical anisotropy of the low-temperature T^2 law of the resistivity, first for a pure lattice and then for an imperfect lattice with an isotropic impurity scattering, as well as the theoretical anisotropy of the magnetic susceptibility at very low temperatures. Using the two wave functions of Refs. 41 and 42, we do not get the correct order for ρ, but with our modified wave function we get the correct order for ρ_0, for the coefficient A of the T^2 term[25] and for the coefficient B of the T term,[21,22] which presents the same anisotropy as the coefficient A. Taking into account the slight high-temperature anisotropy improves the results. It would appear, then, that with the proposed wave function we can identify the scattering at very low temperatures as being Kondo-impurity-like and can then account for the terms quadratic and linear in temperature. The correlation between A and ρ_0 are consistent with this view.

We can also determine theoretically the anisotropy of the thermoelectric power S and the thermal conductivity K. We have computed the low-temperature anisotropy of the thermoelectric power in the case of a pure lattice or in the case of an isotropic impurity scattering and Table VI yields the results for the cerium Kondo compounds that we have previously discussed. We see that, for a

TABLE V. Theoretical values for the coefficients of the T^2 law of the low-temperature resistivity along the three directions for $CeCu_6$, in the case of (i) a pure lattice and (ii) an imperfect lattice with an isotropic impurity scattering. The values of a_0, b_0, and c_0 correspond to the coefficients of the wave function (71) for Refs. 41 and 42 and our proposed wave function, as explained in text. The calculated $T=0$ magnetic susceptibility is also shown in the last columns.

Reference	a_0	b_0	c_0	$A_x^{(i)}$	$A_y^{(i)}$	$A_z^{(i)}$	$A_x^{(ii)}$	$A_y^{(ii)}$	$A_z^{(ii)}$	χ_x	χ_y	χ_z
41	−0.85	+0.37	+0.38	1	1.5	0.6	1	0.9	0.5	1	0.4	27.0
42	−0.73	−0.60	+0.31	1	0.8	0.7	1	1.2	0.9	1	5.0	36.0
Ours	+0.73	−0.60	+0.31	1	0.5	0.7	1	0.97	0.7	1	0.5	3.0

TABLE VI. Theoretical values for the anisotropy of the thermoelectric power at low temperatures, perpendicular to the c axis ($S_\perp$) and parallel to it ($S_\parallel$), calculated for different compounds in the case of (i) a pure lattice and (ii) an imperfect lattice with an isotropic impurity scattering.

Compound	$S_\perp/S_\parallel{}^{(i)}$	$S_\perp/S_\parallel{}^{(ii)}$
$CePt_2Si_2$	1.001	0.53
$CeCu_2Si_2$	1.09	1.83
$CeRu_2Si_2$	1.15	2.61
$CeAl_3$	1.01	0.90
$CeSi_{1.86}$	1.10	1.04

pure lattice, the anisotropy of the linear term in T is very small, the largest value being $S_\perp/S_\parallel=1.15$ for $CeRu_2Si_2$. The anisotropy in the more realistic case when impurity scattering is included is much larger and the values are very close to those obtained for $A_\perp/A_\parallel$ in Table III with the same assumptions. For the thermal conductivity, the anisotropy at $T=0$ when impurity scattering is included is just given by the anisotropy of ρ_0. In both cases, comparison with experiment is difficult, because there are not many available experimental data and moreover there is not a unique behavior at low temperatures. The thermopower has been measured in $CePt_2Si_2$,[18] $CeCu_6$,[22] and $CeRu_2Si_2$ (Ref. 23) single crystals, but there is no clear evidence for a T or T^3 behavior as $T\rightarrow 0$ and, even for a given compound, the behavior is not the same along the different directions. As previously explained in Refs. 18 and 28, our model can account for the experimental tendencies but cannot explain in detail the competition between positive and negative peaks at high temperatures. Finally, the only available experiment on the thermal conductivity K is in $CePt_2Si_2$,[18] where K appears to be linear in T at low temperatures, but we cannot really draw conclusions on this problem.

C. Concluding remarks

Thus, the anisotropy of the transport properties has been accounted for by a model involving primarily crystal-field effects in noncubic cerium Kondo compounds. This has also previously been done for magnetic properties.[27,28] Our theoretical results agree with some experimental data available in compounds such as $CePt_2Si_2$ or $CeCu_6$. In particular, taking into account the disorder first on non-rare-earth sites and then as due to the $4f$ electrons themselves improves in a few cases the agreement with experiment. However, we have not been able to go too far in the quantitative comparison with experiment for at least the two following reasons:

(i) First of all, there is not much available experimental data in single-crystal cerium Kondo compounds and moreover the real influence of the disorder is not clearly established.

(ii) Our theoretical model is simplified, essentially because we consider free conduction electrons with phenomenological effective masses along the principal axes. The assumption of a spherical Fermi surface yields a small anisotropy for the electrical resistivity at high temperatures, which disagrees with some of the experimental data. Our model suffers also from the simplifying assumptions used to describe the disorder.

Thus, the consideration of a more realistic picture for the band structure and disorder will certainly improve the agreement with experiment, but our theoretical model is certainly the first to account for the anisotropy of transport properties in several cerium Kondo compounds.

ACKNOWLEDGMENT

One of us (S.M.M.E.) would like to thank the Royal Society (London) for financial support.

*Present address: Department of Mathematics, Imperial College, 180 Queens Gate, London SW7 2BZ, U.K.

[1]S. M. M. Evans, A. K. Bhattacharjee, and B. Coqblin, Physica B **171**, 293 (1991), and references therein.

[2]B. Barbara, J. X. Boucherle, J. L. Buevoz, M. F. Rossignol, and J. Schweizer, J. Phys. (Paris) Colloq. **40**, C5-321 (1979).

[3]C. Vettier, P. Burlet, and J. Rossat-Mignod, J. Magn. Magn. Mater. **63-64**, 18 (1987).

[4]E. Gratz, E. Bauer, B. Barbara, S. Zemirli, F. Steglich, C. D. Bredl, and W. Lieke, J. Phys. F **15**, 1975 (1985).

[5]R. M. Galera, J. Pierre, E. Siaud, and A. P. Murani, J. Less Common Met. **97**, 151 (1984).

[6]K. Andres, J. E. Graebner, and H. R. Ott, Phys. Rev. Lett. **35**, 1779 (1975).

[7]P. Haen, J. Flouquet, F. Lapierre, P. Lejay, and G. Remenyi, J. Low Temp. Phys. **67**, 391 (1987).

[8]H. R. Ott, H. Rudigier, Z. Fisk, J. O. Willis, and G. R. Stewart, Solid State Commun. **53**, 235 (1985).

[9]R. A. Fisher, S. E. Lacy, C. Marcenat, J. A. Olsen, N. E. Phillips, J. Flouquet, A. Amato, and D. Jaccard, Jpn. J. Appl. Phys. (Suppl. 26-3), **26**, 1257 (1987).

[10]F. Steglich, J. Aarts, C. D. Bredl, W. Lieke, D. Meschede, W. Franz, and H. Schäfer, Phys. Rev. Lett. **43**, 1892 (1979).

[11]B. Cornut and B. Coqblin, Phys. Rev. B **5**, 4541 (1972).

[12]A. K. Bhattacharjee and B. Coqblin, Phys. Rev. B **13**, 3441 (1976).

[13]A. K. Bhattacharjee and B. Coqblin, Phys. Rev. B **38**, 338 (1988).

[14]B. Coqblin and J. R. Schrieffer, Phys. Rev. **185**, 847 (1969).

[15]K. Yamada and Y. Yoshida, Prog. Theor. Phys. **76**, 621 (1986).

[16]A. J. Millis and P. A. Lee, Phys. Rev. B **35**, 3394 (1987).

[17]D. L. Cox and N. Grewe, Z. Phys. B **71**, 321 (1988).

[18]A. K. Bhattacharjee, B. Coqblin, M. Raki, L. Forro, C. Ayache, and D. Schmitt, J. Phys. (Paris) **50**, 2781 (1989).

[19]D. Jaccard, R. Cibin, J. L. Jorda, and J. Flouquet, Jpn. J. Appl. Phys. (Suppl. 26-3) **26**, 517 (1987).

[20]W. Assmus, M. Herrmann, U. Rauchschwalbe, S. Riegel, W. Lieke, H. Spille, S. Horn, G. Weber, F. Steglich, and G. Cordier, Phys. Rev. Lett. **52**, 469 (1984).

[21]A. Sumiyama, Y. Oda, H. Nagano, Y. Onuki, and T. Komatsubara, J. Phys. Soc. Jpn. **54**, 877 (1985).

[22]A. Amato, D. Jaccard, E. Walker, and J. Flouquet, Solid State Commun. **55**, 1131 (1985).

[23]A. Amato, D. Jaccard, J. Sierro, F. Lapierre, P. Haen, P. Lejay, and J. Flouquet, J. Magn. Magn. Mater. **76-77**, 263 (1988).
[24]R. M. Marsolais, C. Ayache, D. Schmitt, A. K. Bhattacharjee, and B. Coqblin, J. Magn. Magn. Mater. **76-77**, 269 (1988).
[25]Y. Onuki, Y. Shimizu, and T. Komatsubara, J. Phys Soc. Jpn. **54**, 304 (1985).
[26]B. Coqblin, A. K. Bhattacharjee, and S. M. M. Evans, J. Magn. Magn. Mater. **90-91**, 393 (1990).
[27]S. M. M. Evans, J. Phys. Condens. Matter **2**, 9097 (1990).
[28]S. M. M. Evans and B. Coqblin, Phys. Rev. B **43**, 12 790 (1991).
[29]S. Kashiba, S. Maekawa, S. Takahashi, and M. Tachiki, J. Phys. Soc. Jpn. **55**, 1341 (1986).
[30]S. Maekawa, S. Kashiba, M. Tachiki, and S. Takahaski, J. Phys Soc. Jpn. **55**, 3194 (1986).
[31]J. Rasul and H. U. Desgranges, J. Phys. C **19**, L671 (1986).
[32]P. Coleman, Phys. Rev. B **29**, 3055 (1984).
[33]N. Read and D. M. Newns, Solid State Commun. **52**, 993 (1984).
[34]S. Zhang and P. M. Levy, Phys. Rev. B **40**, 7179 (1989).
[35]D. Jaccard, R. Cibin, and J. Sierro, Helv. Phys. Acta **61**, 530 (1988).
[36]J. M. Lawrence, J. D. Thomson, and Y. Y. Chen, Phys. Rev. Lett. **54**, 2537 (1985).
[37]E. P. Fetisov and D. I. Khomskii, Zh. Eksp. Teor. Fiz. **92**, 105 (1987) [Sov. Phys. JETP **65**, 59 (1987)].
[38]M. Raki, L. Forro, C. Ayache, D. Schmitt, A. K. Bhattacharjee, and B. Coqblin, Physica B **163**, 93 (1990).
[39]F. Lapierre and P. Haen (unpublished).
[40]J. Pierre, O. Laborde, E. Haussay, A. Rouault, J. P. Senateur, and R. Madar, J. Phys. Condens. Matter **2**, 431 (1990).
[41]S. Takayanagi, Y. Onuki, and T. Komatsubara, J. Phys. Soc, Jpn. **55**, 2384 (1986).
[42]S. Zemirli and B. Barbara, Solid State Commun. **56**, 385 (1985).